

Received by OSTI

JUL 9 8 1987

CONF-8609296--1

RECENT RESULTS ON POLARIZATIONS AND THE PRESENT STATUS OF

THE FERMILAB POLARIZED BEAMS[§]

ANL-HEP-CP--87-31

Akihiko Yokosawa

DE87 011405

High Energy Physics Division
Argonne National Laboratory, Argonne, Illinois

There are two sections in this paper. In the first section we discuss the nucleon-nucleon scattering at intermediate energies including the present status of dinucleon resonances. In the second section we present the Fermilab polarized-beam program.

I. Recent Results on Polarizations in Nucleon-Nucleon Scattering

We review experimental results concerning polarization phenomena in nucleon-nucleon scattering at intermediate energies, and the present status of $S = 0$ dibaryon resonances.

A) Introduction

We review new experimental results including the data taken with the Argonne ZGS polarized-proton beams. These results continue to have an impact on the field of polarization phenomena. Many structures were found at lower energies, up to about 4-GeV/c incident proton momentum. Remarkable spin

MASTER

[§] Work supported by the U.S. Department of Energy, Division of High Energy Physics, Contract W-31-109-ENG-38.

psw

effects were observed in the spin-spin correlation measurements up to 12 GeV/c. It is also attempted to update an earlier paper on the nucleon-nucleon polarization phenomena.¹

B) pp Scattering Amplitude Measurements

Results of measurements on a number of triple- and double-spin correlation parameters in proton-proton elastic scattering at 6 GeV/c over the $|t|$ range between 0.2 and 1.0 (GeV/c)² were recently published.² These new data permit the first nucleon-nucleon amplitude determination above the "dibaryon resonances" region. A total of 14 different spin observables were measured (five spin transfer, four depolarization, and five triple-spin correlation parameters). These have been combined with earlier results, resulting in 20 different spin observables for each of six $|t|$ values between 0.2 and 1.0 (GeV/c)². A solution for the amplitudes has been found at each $|t|$. The amplitudes are normalized so that $d\sigma/d\Omega = 1$.

Here we define scattering amplitudes in two different ways:³

1) s-channel helicity amplitudes

$$\langle ++ | -- \rangle = \phi_1$$

$$\langle -- | ++ \rangle = \phi_2$$

$$\langle +- | +- \rangle = \phi_3$$

$$\langle +- | -+ \rangle = \phi_4$$

$$\langle ++ | +- \rangle = \phi_5$$

2) t-channel exchange amplitudes (N_0 , N_1 , N_2 , U_0 , and U_2 which have definite quantum numbers exchanged at asymptotic energy)

Natural-parity exchange:

$$N_0 = 1/2 (\phi_1 + \phi_3), N_1 = \phi_5, N_2 = 1/2 (\phi_4 - \phi_2)$$

Unnatural-parity exchange:

$$U_0 = 1/2 (\phi_1 - \phi_3), U_2 = 1/2 (\phi_2 + \phi_4)$$

Cross section:

$$d\sigma/d\Omega = |N_0|^2 + 2|N_1|^2 + |N_2|^2 + |U_0|^2 + |U_2|^2$$

(the subscripts correspond to the total s-channel helicity flip).

The results of the amplitude determination are shown in Fig. 1a for the exchange amplitudes and in Fig. 1b for the s-channel helicity amplitudes.² Note that the magnitudes of N_0 , ϕ_1 , and ϕ_3 are scaled down a factor of 5 in

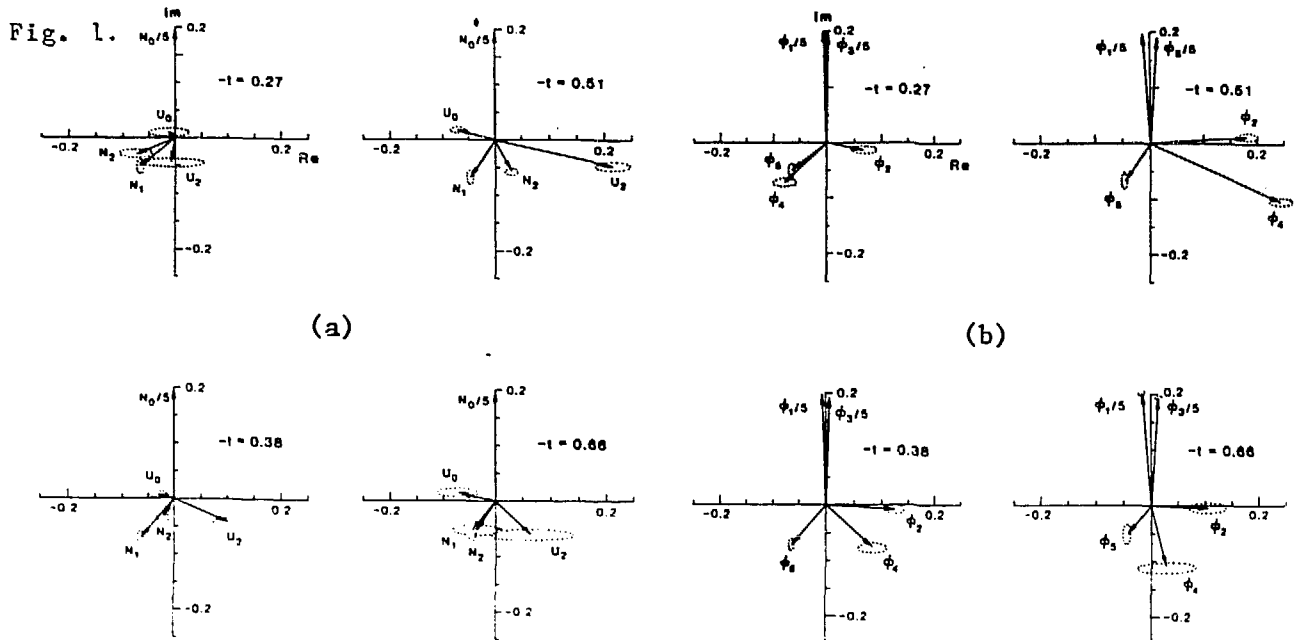


Fig. 1a. pp scattering amplitudes at 6 GeV/c (exchange channel).
 Fig. 1b. pp scattering amplitudes at 6 GeV/c (s-channel helicity channel).

In particular, the data show that the spin non-flip helicity amplitudes ϕ_1 and ϕ_3 are much larger than the spin-flip amplitudes. This indicates that helicity conserving exchange terms are dominant, as would be the case if exchanged gluons couple to current quarks in the nucleons. The amplitude picture seems easier to understand in terms of the s-channel helicity amplitudes, where little variation is observed in ϕ_1 , ϕ_3 , and ϕ_5 over most of the t-range of this experiment. As noted above, the dominant amplitudes are $\phi_1 \approx \phi_3$. In addition, the ϕ_2 amplitude remains almost real though there is a change in its magnitude. There is, however, a large variation in both the magnitude and direction of ϕ_4 . As has been noted by Kroll et al.,⁴ "surprisingly, the most interesting structure is in ϕ_2 and ϕ_4 themselves rather than in the combinations N_2 and U_2 ".

Various recent theoretical activities for the scattering amplitudes are summarized here. It is hoped that the new data will stimulate further work. The classical Regge description and predictions were in general agreement with the data.⁵ Wakaizumi et al.⁶ investigated the pp interaction at 6 and 12 GeV/c at all angles using the impact-parameter representation and the eikonal model. Fits to previous data allowed conclusions on the magnitude of the short-, medium-, and long-range components of the spin dependent eikonals. Semiphenomenological phase-shift analyses⁷ were performed at 6 GeV/c. Moravcsik, Goldstein, and coworkers have commented on pp elastic scattering at 6 GeV/c in many articles.⁸⁻¹³ Several papers deal with the problem of how best to determine the amplitudes.^{8,9,14} An extensive amplitude analysis from $|t| = 0.05$ to 1.0 (GeV/c)² was also performed.^{8,11} Polarization tests of one-particle-exchange mechanisms were applied to the 6-GeV/c amplitudes and were shown to be satisfied, whereas they failed at lower energies.¹² Finally, these

authors also try to interpret the results for the 6-GeV/c amplitudes in the framework of QCD.¹³

C) pp Elastic Scattering at Large Angles

The spin-correlation parameters at $p_{\perp} > 2$ GeV/c are given in measurements of C_{NN} (A_{NN}) = (N,N;0,0) and C_{LL} = (L,L;0,0) at 11.75 GeV/c covering large c.m. scattering angles.^{15,16} The results are shown in Fig. 2. At $\theta_{c.m.} = 90^{\circ}$, one can obtain the value of C_{SS} from the relationship, $C_{NN} - C_{SS} - C_{LL} = 1$. The parameters C_{NN} and C_{SS} at $\theta_{c.m.} = 90^{\circ}$ are expressed in terms of s-channel helicity amplitudes as

$$C_{NN} = \text{Re}(\phi_1^* \phi_2 - \phi_3^* \phi_4) / \sigma$$

and

$$C_{SS} = \text{Re}(\phi_1^* \phi_2 + \phi_3^* \phi_4) / \sigma.$$

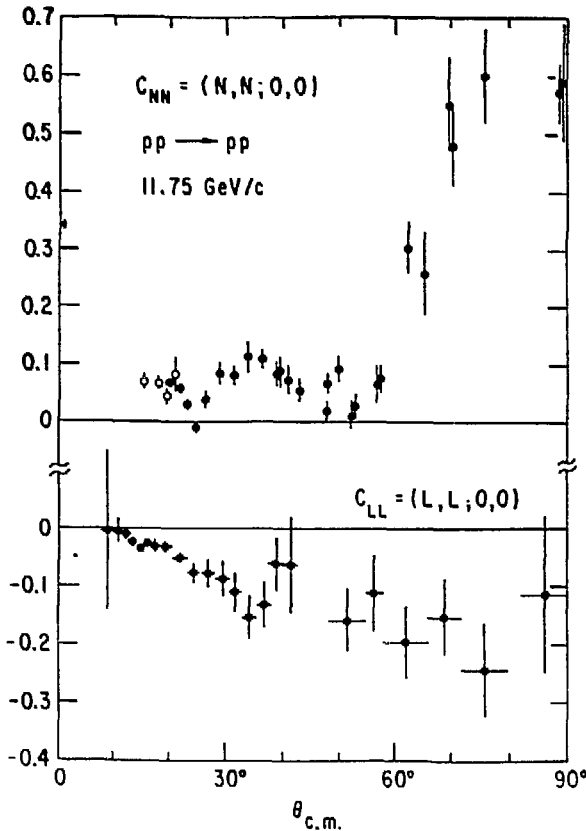


Fig. 2.

C_{NN} (A_{NN}) and C_{LL} at 11.75 GeV/c at large angles.

For the data with $p_{\perp} > 2$ GeV/c we attempt to test the helicity conservation among the quarks¹⁷ based upon the assumption that the proton spins made from

quarks and quark mass ≈ 0 is the most important one. The helicity conservation requires that the helicity flip amplitudes must vanish as

$$\phi_2 = \langle -- | ++ \rangle = 0, \text{ and}$$

then $C_{NN} = -C_{SS}$. The experimental data at $\theta_{c.m.} = 90^\circ$ show that $C_{NN} = 0.57 \pm 0.08$ and $C_{SS} = -0.30 \pm 0.16$. The results imply that we observe approximately helicity conservation among the quarks.

The energy dependence of C_{NN} , C_{LL} , and C_{SS} at $\theta_{c.m.} = 90^\circ$ is predicted up to $p_{lab} = 12$ GeV/c by viewing the reaction amplitudes in the planar-transverse frame.¹⁸

An asymmetry measurement in $pp^\dagger \rightarrow pp$ elastic scattering at Brookhaven¹⁹ yielded high values (up to $\sim +25\%$) of the polarization parameter at $p_\perp > 2$ GeV/c. J. Soffer et al. describe the results in terms of soft- and hard-collision processes.²⁰

D) C_{SS} , C_{LS} , and C_{LL} Measurements at 11.75 GeV/c

Recently results of various spin parameters in the pp elastic scattering at 11.75 GeV/c were published.²¹ The measurements of parameters $C_{SS} = (S,S;0,0)$ and $C_{LS} = (L,S;0,0)$ for $\theta_{c.m.} = 8^\circ - 49^\circ$, and of $C_{LL} = (L,L;0,0)$ for $\theta_{c.m.} = 8^\circ - 90^\circ$ were performed as shown in Fig. 3. We note that results of the spin parameter $C_{NN} = A_{NN} = (N,N;0,0)$ were published earlier.²²

E) Nucleon-Nucleon Scattering at Intermediate Energies and Present Status of Dibaryon-Resonance

1) Introduction

Most of the experimental results in nucleon-nucleon scattering at intermediate energies are related to "resonant-like" structures. Here we will discuss the nucleon-nucleon scattering which impacts on the structures.

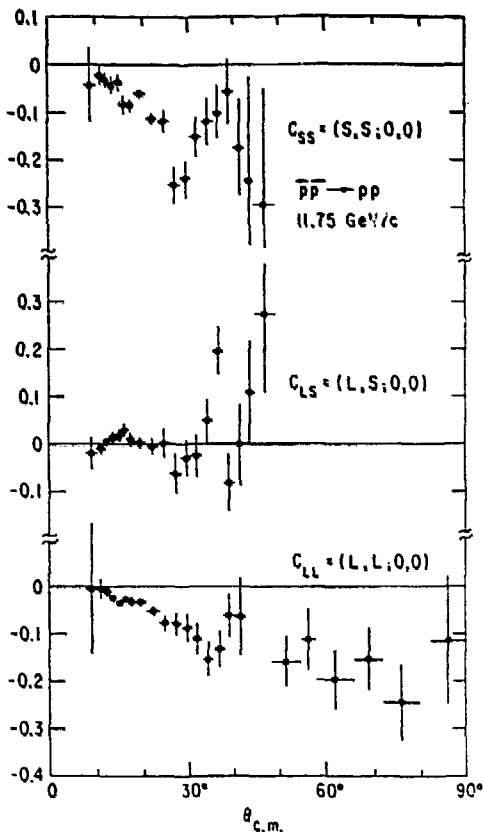


Figure 3

Pure spin-spin correlation parameters C_{SS} , $C_{LS} = C_{SL}$, and C_{LL} as measured by this experiment for pp elastic scattering at 11.75 GeV/c laboratory beam momentum. Data from all settings have been combined and corrected for the presence of other spin parameters as described in the text.

For nearly one decade, an extensive search for dibaryon resonances in the various reactions in the NN, πd , γd , and other channels has been made. A summary on this subject has been described earlier¹ and here we concentrate on relatively new data. Many structures were found in the NN system and they were investigated by means of phase-shift analyses. The results confirmed Breit-Wigner behavior for some of them. Structures observed in the NN, πd , and γd channels are not explained by the standard theories, with the exception of some phenomenological models, and are well explained by adding the dibaryon admixture to theoretical models.

As evidence for the existence of dibaryons grows, it becomes crucial to understand the nature of these resonances. Earlier references to theoretical work (MIT bag model, string model, spring model, πNN and $\pi\pi NN$ dynamics, Deck model, OPE three-body theory, OBE inelastic-threshold model, coupled-channels method etc.) were discussed in Ref. 3. Recent references are discussed in

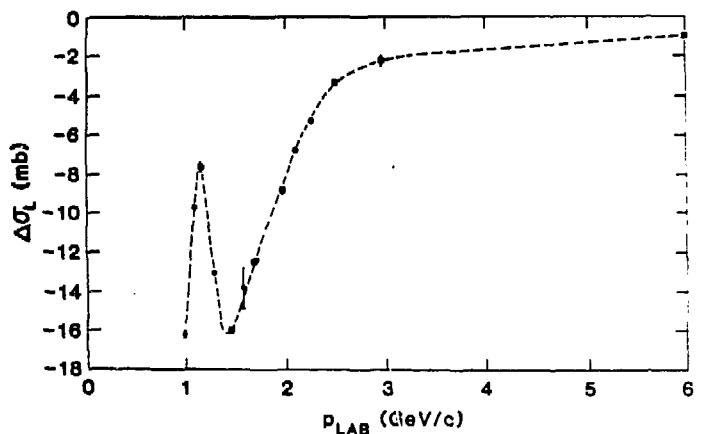
this paper. One nice way to clarify the nature of resonances is to thoroughly study the isospin-zero channels in the region where there is no Δ excitation. Structures were seen in the existing $\Delta\sigma_L(I = 0)$ data, although these are yet to be confirmed. We are expecting various experimental data in this channel in a few years.

We start with discussing structures in the NN channel and compare these with structures in other channels (πd , γd , etc.).

2) I = 1 System

We previously summarized measurements of the difference between the pp total cross sections for parallel and antiparallel spin states, $\Delta\sigma_L = \sigma^{\text{Tot}}(\uparrow\uparrow) - \sigma^{\text{Tot}}(\uparrow\downarrow)$, using a longitudinally polarized beam and target up to 6.00 GeV/c.¹ The ZGS data, including the estimated Coulomb-nuclear (C-N) interference process, of Ref. 3 are shown in Fig. 4. The dip and peak structures have been interpreted as evidence for the formation of diproton resonances, $B_1^2(2.14)$ with a quantum state of 1D_2 and $B_1^2(2.22)$ with 3F_3 state.¹ We attempted to look for additional $\Delta\sigma_L$ structure in the momentum region higher than those previously found and the results²³ obtained are shown in Fig. 5. The errors shown are purely statistical; systematic errors are estimated to be 6% of $\Delta\sigma_L$. We have neglected Coulomb-nuclear interference effects, which depend on spin-spin correlations. We believe these effects are small.²⁴

Fig. 4 $\Delta\sigma_L$ vs. p_{lab} up to 6 GeV/c from previous data. The Coulomb-nuclear (CN) interference correction was included. The dashed curve is only to guide the eye.



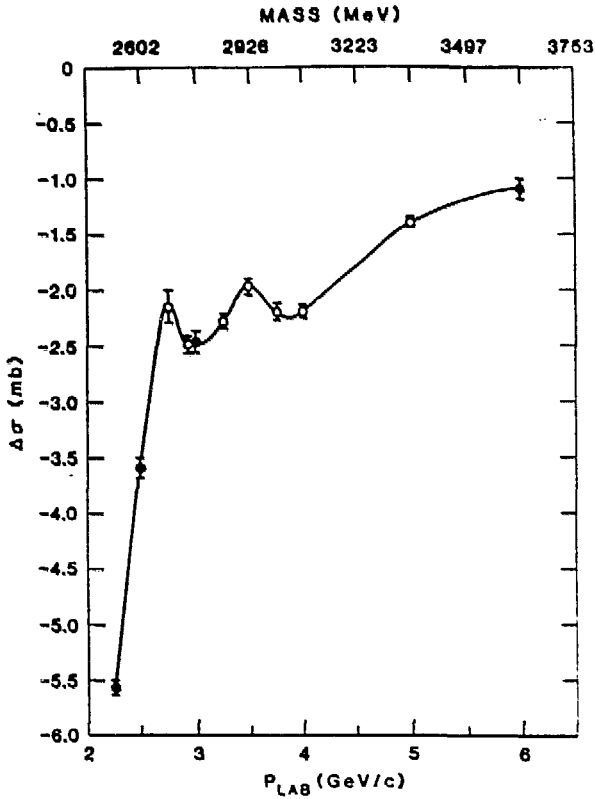


Fig. 5

The $\Delta\sigma_L$ Dependence on p_{lab} .

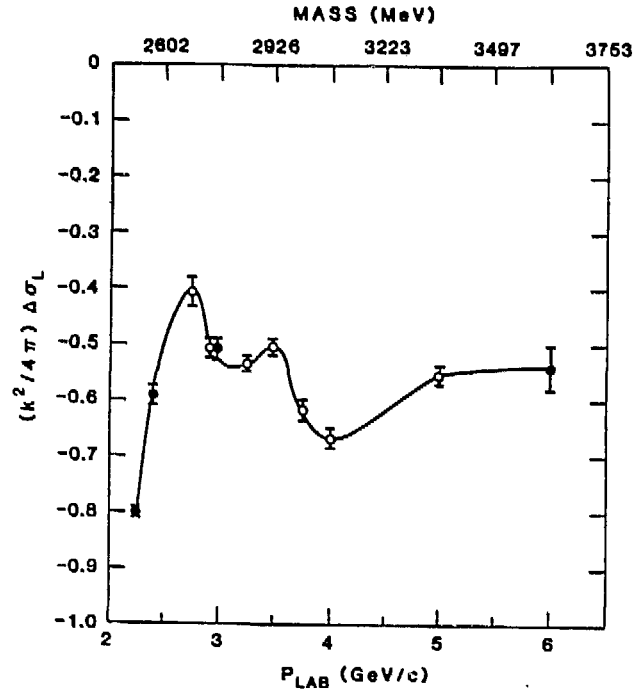


Fig. 6

A plot of $(k^2/4\pi) \Delta\sigma_L$.

Line drawn is only to guide the eye.

To study the behavior in terms of the partial scattering amplitudes, the data on the dimensionless quantity $(k^2/4\pi) \Delta\sigma_L$ are plotted in Fig. 6 as a function of the center-of-mass energy, where k is c.m. momentum. $\Delta\sigma_L$ can be expressed as

$$\Delta\sigma_L = (4\pi/k) \text{Im}[\phi_1(0) - \phi_3(0)] \quad (1)$$

and the spin-averaged cross section as

$$\sigma^{\text{Tot}} = (2\pi/k) \text{Im}[\phi_1(0) + \phi_3(0)]. \quad (2)$$

When the helicity amplitudes are decomposed into partial waves,

$$\text{Im}\phi_1(0) = \frac{1}{k} \sum_J \text{Im}\{(2J+1)R_J + (J+1)R_{J+1,J} + JR_{J-1,J} + 2[J(J+1)]^{1/2}R^J\}, \quad (3)$$

$$\text{Im}\phi_3(0) = \frac{1}{k} \sum_J \text{Im}\{(2J+1)R_{JJ} + JR_{J+1,J} + (J+1)R_{J-1,J} - 2[J(J+1)]^{1/2}R^J\}, \quad (4)$$

where R_J is the spin-singlet partial-wave with $J = L = \text{even}$, R_{JJ} and $R_{J\pm 1,J}$ are spin-triplet waves with $J = L = \text{odd}$ and $J = L \mp 1 = \text{even}$, respectively, and R^J is the mixing term. (Note that $R_J = (\eta_J e^{i2\delta_J} - 1)/i2k$, and similarly for triplet waves).

If the bumps in $(k^2/4\pi) \Delta\sigma_L$ are considered to be due to resonances, one of them at 2.75 GeV/c is about mass of 2700 MeV with a width of less than 80 MeV and an elasticity, η , of more than 0.10 for R_J assuming $J = 0$ or for $R_{J+1,J}$ as one can see from Eqs. 1, 3, and 4 along with Fig. 6. The mass of the second bump is about 2900 MeV.

Earlier, structures near 2700 MeV and 2900 MeV were observed in the spin-spin correlation parameter $C_{LL} = (L,L;0,0)$ in p-p elastic scattering around $\theta_{\text{c.m.}} = 90^\circ$.²⁵ Also a strong energy dependence including a shoulder around the 2700-MeV mass region has been observed in a plot of $k^2 C_{NN} (d\sigma/d\Omega)$, where $C_{NN} = (N,N;0,0)$, at $\theta_{\text{c.m.}} = 90^\circ$.³

Polarization measurements for $p^{\uparrow}p \rightarrow d\pi^{\uparrow}$ from $T_p = 1.0$ to 2.3 GeV carried out at Saclay revealed a structure near $T_p \approx 1.9$ GeV (near 2700-MeV mass).²⁶ Recently, structures found in π^-d elastic scattering²⁷ in the backward region were interpreted as the manifestation of the dibaryon resonance with the mass of 2900 MeV.²⁸ Phenomenological analysis allows us to define quantum number of $B_1^2(2900)$ as well as the partial widths of its decay into different channels.

We note that the Cloudy Bag model^{29,30} predicts six-quark state resonances, and in particular an s-wave state near 2700-MeV mass with ~ 50 MeV width²⁹ may be consistent with the new structure.

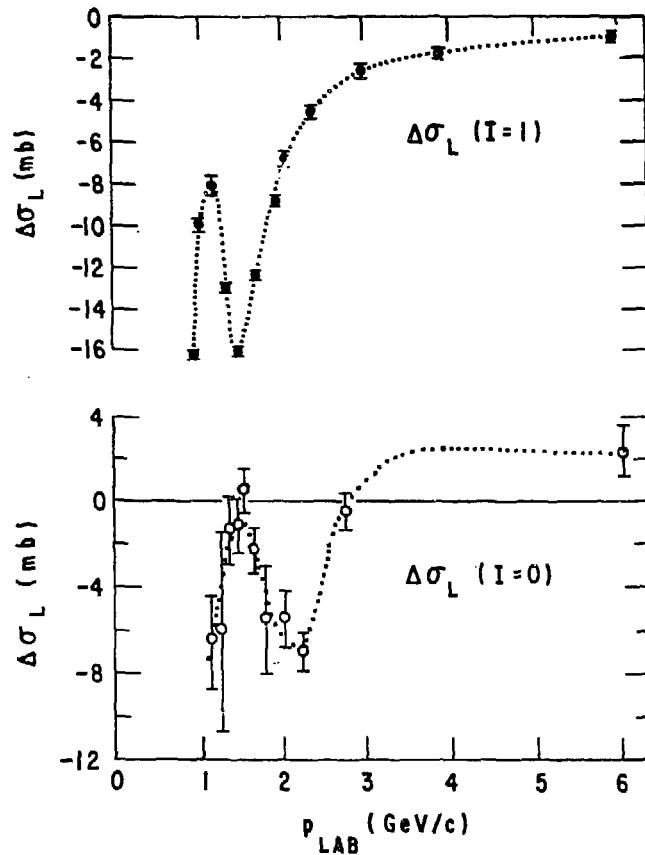
It is highly desirable to measure both $\Delta\sigma_L$ and $\Delta\sigma_T$ in this mass region with smaller energy steps (≈ 20 MeV).

3) Preliminary Results for $C_{TL}(pp)$ and $C_{TL}(np)$

Measurements of the difference between isoscalar nucleon-nucleon total cross sections for pure longitudinal initial spin states, $\Delta\sigma_L(pd)$, were performed using a polarized proton beam and a polarized deuteron target.³¹ One can extract $\Delta\sigma_L(I=0)$ data using both $\Delta\sigma_L(pd)$ and $\Delta\sigma_L(pp)$ as shown in Fig. 7. A significant structure is observed around 1.5 GeV/c. From the dispersion analysis of a forward $I=0$ scattering amplitude using the data on $\Delta\sigma_L(I=0)$, Grein and Kroll³² showed that the Argand plot of the amplitude has a resonance-like behavior around 1.5 GeV/c.

Fig. 7

$\Delta\sigma_L(I=0)$ together
with $\Delta\sigma_L(I=1)$.



The polarization parameters of the pn elastic scattering were measured at KEK covering beam momenta from 1.30 to 1.82 GeV/c.³³ The data are consistent with earlier predictions of the resonant-like behavior in singlet state 1F_3 (2190).³⁴ Measurements of many other parameters are obviously needed for the $I = 0$ phase-shift analyses.

An extensive study³⁵ on the $I = 0$ system is being undertaken at LAMPF (Los Alamos) using polarized neutron beams.³⁶ A longitudinally polarized neutron beam is produced at forward angles when a longitudinally polarized proton beam strikes a deuteron target. In the energy interval of 500 to 800 MeV polarization value is $\sim 50\%$. The measurements include n-p elastic-scattering observables C_{SS} , C_{LS} , C_{LL} etc. of a wide angular range at energies of 500, 650, and 800 MeV. Preliminary data show that predictions from presently available np phase-shift solutions are rather good. The total cross section measurements with spin will also be performed. We expect the experimental results will clarify the structure in $I = 0$ system.

We note that the np total cross-section data show no evidence for narrow resonances in a mass range below 2.23 GeV.³⁷

II) The Present Status of the Fermilab Polarized Beams

A) Introduction

During the last decade, construction of a high-energy (above 100 GeV/c) polarized beam has been attempted. In order to avoid possible complications involving depolarization at high energies, polarized protons are produced from decaying lambdas. The Fermilab polarized-beam facility is expected to be operational within the next several months.

B) Construction of Polarized Beam

We review the earlier design of the polarized-proton beam at CERN.¹ The idea then was to select high-momentum protons which were forward decaying, around $\theta_{c.m.} = 0^\circ$, from lambdas near the highest momentum point of the lambda production spectrum. These protons were longitudinally polarized. However, this method could not be applied to either low-momentum protons produced using 1-TeV incident protons or antiprotons since antilambdas are produced at much lower momenta than the incident momentum of protons striking a production target.

It has been shown that we can select protons or antiprotons which are decaying around $\theta_{c.m.} = 90^\circ$.² We show how this scheme works.

The polarization of protons and antiprotons comes from parity violating decays of lambdas and antilambdas respectively, and the measured polarization was 64%.³ The spin direction in the antilambda center-of-mass frame (decay frame) is shown in Fig. 1.

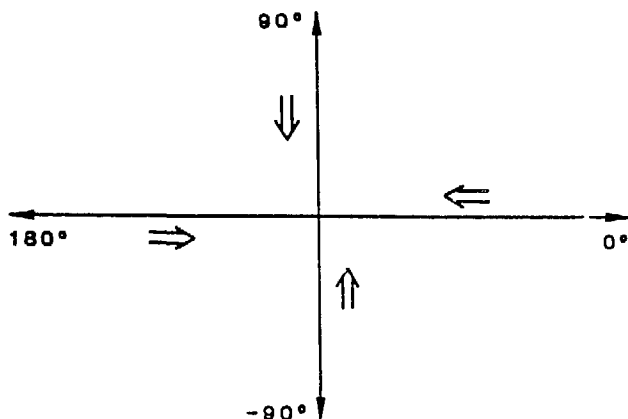


Figure 1 Spin direction of anti-protons vs. decay angles. The spin direction is indicated by \ddagger and $\uparrow\uparrow$ symbols.

We note that spin direction is almost unchanged in transforming from the lambda decay frame to the laboratory. Therefore protons and antiprotons with $\theta_{c.m.} = 0^\circ$ and 180° are longitudinally polarized (\vec{L}) while those with $\theta_{c.m.} = 90^\circ$ are transversely polarized (\vec{N} or \vec{S}) in the laboratory. Since protons and antiprotons with $\theta_{c.m.} = 0^\circ$ and 180° move in the same direction (lab decay angle = 0°) in the laboratory, there are no longitudinally polarized beams at momenta which are much less than the incident proton momentum.

Protons with $\theta_{c.m.} = 90^\circ$ and -90° have the opposite laboratory decay angles which are not zero. They can be distinguished from those decaying at $\theta_{c.m.} = 0^\circ$ from lambda with the production target as the source of the beam. Virtual sources for $|\theta_{c.m.}| = 90^\circ$ particles are illustrated in Fig. 2. The spin direction, \vec{N} or \vec{S} , should be chosen using the field direction of the bending magnet, so that the spin direction is parallel to the field. The polarized beam line (up to 200 GeV/c) at Fermilab is shown in Fig. 3. Here we produce the \vec{S} type beam before reaching the snake magnets. The estimated intensities of polarized beams with a beam polarization of 45% produced by 400-GeV/c and 1000-GeV/c incident protons are shown in Fig. 4.

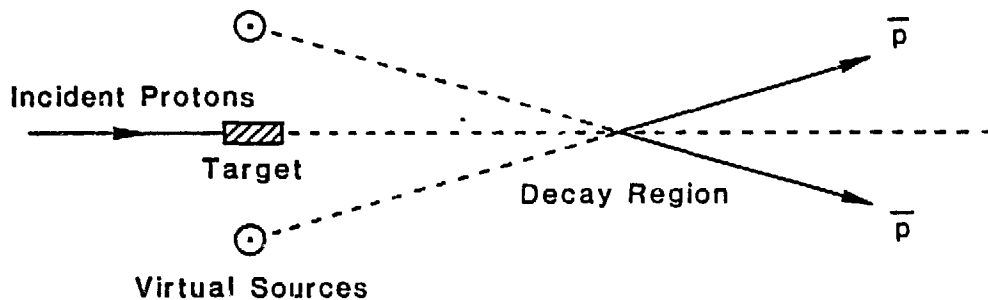


Figure 2 Virtual Sources

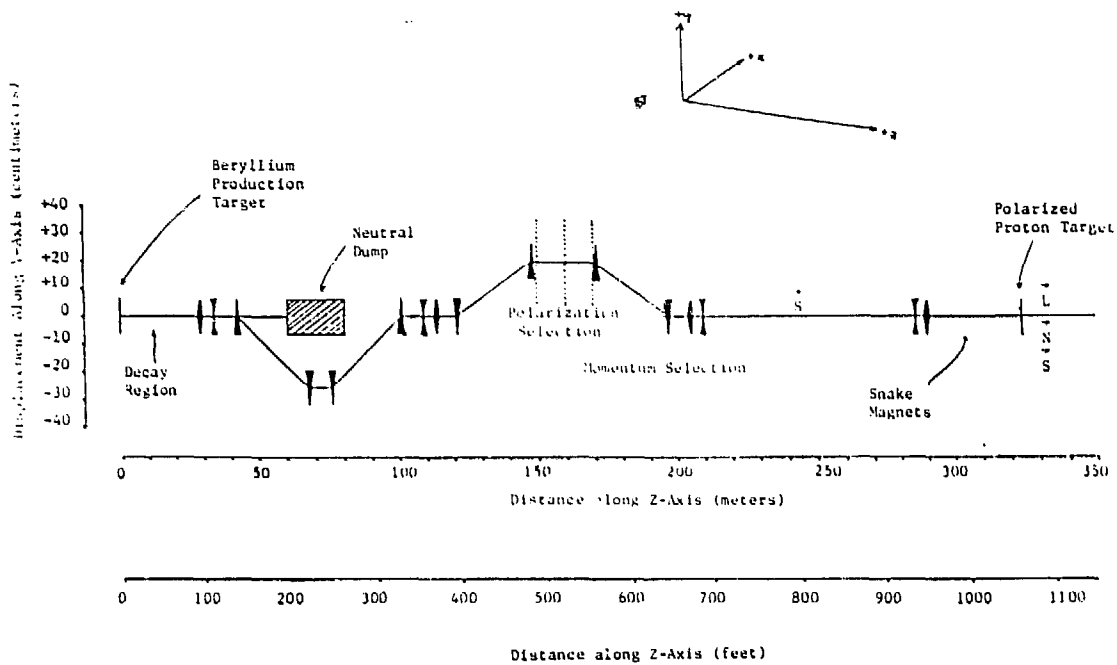


Figure 3 Side View of Fermilab Polarized Beam

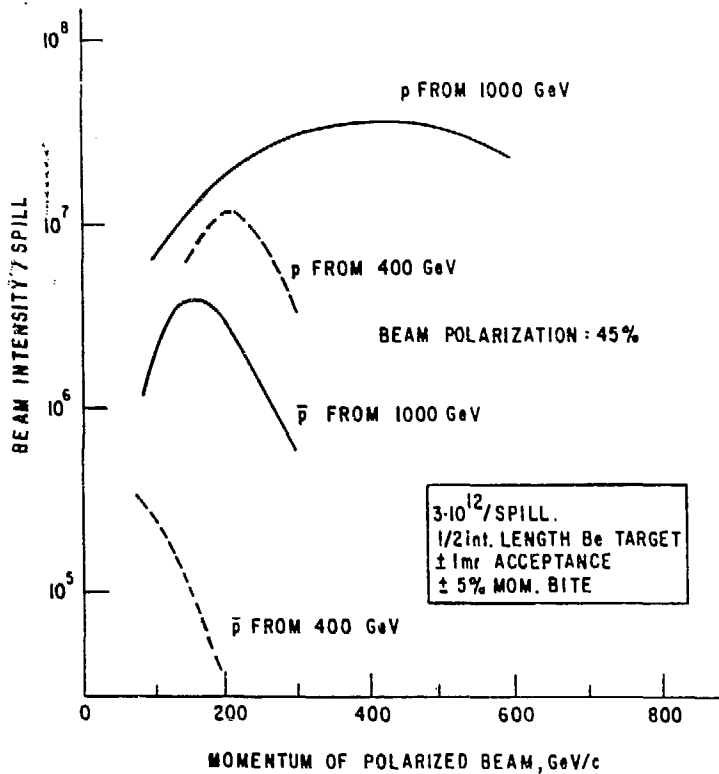


Figure 4
Polarized Beam Intensity

The very first measurement we need to carry out is to determine the polarization of the polarized beams. We describe two polarimeters currently being installed in the experimental hall.

1) Coulomb-Nuclear Polarimeter

This is to measure the interference term of the non-flip amplitude and the electromagnetic spin-flip amplitude. The proton polarization arising from the interference is $P \approx 5\%$ at $|t| \approx 2 \cdot 10^{-3} (\text{GeV}/c)^2$ and is energy independent.

2) Primakoff-Effect Polarimeter

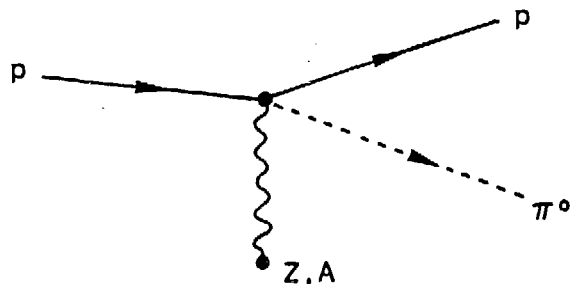
This is to apply the results of the low-energy processes, which are related to the low-momenta high energy reactions. The diffractive dissociation of incoming proton into (πN) system by the Coulomb field⁴ of nuclei seems the most promising channel as proposed by Underwood.⁵ This scheme is shown in Fig. 5. The process $pA \rightarrow pA\pi^0$ can be related via the Primakoff effect to low-energy photoproduction, i.e., $\gamma p \rightarrow \pi^0 p$. The amplitude ψ for diffractive production from a nucleus with charge Z and atomic number A can be written as:

$$\int |\psi|^2 d\phi = \frac{Z^2 \alpha}{2} \left(\frac{2M_A}{s_{\pi p} - m_p^2} \right)^2 \left(A \cdot \frac{d\sigma}{d\Omega} \right)_{\gamma p \rightarrow \pi^0 p},$$

where A is the photoproduction asymmetry at the given value of p_{\perp} and $s_{\pi p}$. Asymmetries at the γp kinetic energy of 600 MeV are as large as 60%.

Figure 5

Primakoff Effect



C) Experimental Program

Experiment 704, the Integrated Proposal on First Round Experiments with the Polarized Beam Facility, constitutes a proposal to simultaneously perform substantial parts of previously proposed Experiments 674 (Asymmetries in Inclusive Pion and Kaon Production at Large x with a Polarized Beam), 676 (An Experiment to Measure $\Delta\sigma_L$ in p - p and \bar{p} - p Scattering Between 100 and 500 GeV), 677 (To Study the Spin Dependence in the Inclusive Production of Lambda Particles with the Polarized Beam), and 678 (Proposal to Study the Spin Effects in Inclusive π^0 and Direct Gamma Production at High- p_{\perp} with the Polarized Beam Facility).

Experimenters involved in these measurements are from Argonne National Laboratory, Fermilab, Kyoto University (Japan), LAPP (Annecy, France), Los Alamos National Laboratory, Northwestern University, Rice University, CEN Saclay (France), IHEP-Serpukhov (USSR), University of Texas, and Trieste (Italy).

The integrated proposal is for a 200-GeV/c conventional magnet beam line. We will carry out the following measurements:

1) $\Delta\sigma_L(pp)$ and $\Delta\sigma_L(\bar{p}p)$

We intend to explore the spin dependence of the interactions in a global way using a straightforward experiment which will measure the difference in pp and $\bar{p}p$ total cross sections between the states with helicities of target and beam parallel and antiparallel. Experience shows that accuracy of ± 100 microbarns can easily be achieved.

2) $p \uparrow p \rightarrow \pi^0, \pi^{\pm}, \Lambda^0, \Sigma^0$

We will simultaneously study the inclusive production of neutral pions around $x_F \approx 0$ at large p_{\perp} , and of Λ^0, Σ^0 at large x . Interpretation of the polarization of Λ^0 produced inclusively ($pp \rightarrow \Lambda^0 \uparrow_x, Kp \rightarrow \Lambda^0 \uparrow_x$) has given rise

to extensive discussion about the origin of this polarization. We expect that information of spin transfer from initial to final state in this reaction will enlighten the debate.

The major detectors for this experiment are: two gamma spectrometers with 500 lead-glass cells each will be used to detect γ 's from π^0 decay. The magnetic spectrometer with proportional and drift-chamber systems and with a Cerenkov counter is to detect π^\pm , Λ^0 , and Σ^0 .

The technique for measuring single spin measurements in hadron production is considerably improved over the previous experiment since the polarized beam allows the use of a liquid hydrogen target.

Pending proposals using the polarized-beam facility are:

- #682 Study of the P_\perp Dependence of π^\pm Inclusive Production with a Polarized Proton Beam and Target
- #688 Nuclear-Size Dependence of Single-Spin Asymmetries in High- p_\perp Hadron Production
- #699 Study of Spin-Dependent Asymmetries Using Calorimeter Triggered High- p_\perp Events with Polarized Beam and Polarized Target.

REFERENCES (Section I)

- 1) A. Yokosawa, Proc. Sixth Int. Symp. Polar. Phenom. in Nucl. Phys., Osaka, (1985), (J. Phys. Soc. Jpn. 55 (1986) Suppl. p. 251-271), and references therein.
- 2) I. P. Auer et al., Phys. Rev. D32, 1609 (1985).
- 3) A. Yokosawa, Phys. Reports 64, (1980); and references therein.
- 4) P. Kroll, E. Leader, and W. von Schlippe, J. Phys. G4, 1003 (1978).
- 5) E. L. Berger et al., Phys. Rev. D17, 2971 (1978).
- 6) S. Wakaizumi and M. Sawamoto, Prog. Theor. Phys. 64, 1699 (1980);
S. Wakaizumi, Prog. Theor. Phys. 67, 531 (1982).
- 7) M. Matsuda et al., Prog. Theor. Phys. 62, 1436 (1979); 64, 1344 (1980).
- 8) N. Ghahramany et al., Phys. Rev. D28, 1086 (1983).
- 9) G. R. Goldstein and M. J. Moravcsik, Phys. Lett. 102B, 189 (1981);
Ann. Phys. (NY) 142, 219 (1982); K. Nam et al., Phys. Rev. Lett. 52, 2305
(1984).
- 10) M. J. Moravcsik et al., Phys. Rev. D30, 1899 (1984).
- 11) N. Ghahramany et al., Phys. Rev. D31, 195 (1985).
- 12) G. R. Goldstein and M. J. Moravcsik, Phys. Rev. D30, 55 (1984);
G. R. Goldstein et al., Phys. Lett. 152B, 265 (1985).
- 13) G. R. Goldstein and M. J. Moravcsik, to be published.
- 14) P. W. Johnson et al., Phys. Rev. D15, 1895 (1977); D16, 2783 (1977).
- 15) D. G. Crabb et al., Phys. Rev. Lett. 41, 1257 (1978); E. A. Crosbie
et al., Phys. Rev. D23, 600 (1981).
- 16) I. P. Auer et al., Phys. Rev. Lett. 52, 808 (1984).

- 17) For instance, see S. J. Brodsky and G. P. Lepage, Phys. Rev. D24, 2848 (1981).
- 18) F. Arash et al., to be published in Phys. Rev. Comm. D.
- 19) P. R. Cameron et al., to be published.
- 20) C. Bourrely and J. Soffer, Phys. Rev. Lett. 54, 760 (1985).
- 21) I. P. Auer et al., Phys. Rev. D34, 1 (1986).
- 22) E. A. Crosbie et al., Phys. Rev. D23, 600 (1981), and references therein
- 23) I. P. Auer et al., Phys. Rev. D34, 2581 (1986); I. P. Auer et al. to be published
- 24) I. P. Auer et al., Phys. Rev. Lett. 41, 354 (1978)
- 25) I. P. Auer et al., Phys. Rev. Lett. 48, 1150 (1982).
- 26) R. Bertini et al., Saturne-Lyon-Orsay-Alberta Collaboration.
- 27) B. M. Abramov et al., Nucl. Phys. A372, 301 (1981); B. M. Abramov et al., Preprint ITEP, No. 160 (1985).
- 28) I. V. Chuvilo et al. ITEP, No. 164 (1986).
- 29) E. L. Lomon, Nucl. Phys. A434, 139C-150C (1985).
- 30) P. J. Mulders and A. W. Thomas, J. Phys. G9, 1159 (1983).
- 31) I. P. Auer et al., Phys. Rev. Lett. 46, 1177 (1981).
- 32) W. Grein and P. Kroll, Nucl. Phys. A377, 505 (1982).
- 33) M. Sakuda et al., Phys. Rev. D25, 2004 (RC) (1982).
- 34) K. Hashimoto et al., Prog. Theor. Phys. 64, 1678 (1980); 64, 1693 (1980).
- 35) LAMPF elastic-scattering experiments E-665/770, and E-589/861, followed by E-683, $\Delta\sigma_L$ and $\Delta\sigma_T$ measurements.
- 36) J. S. Chalmers et al., Phys. Lett. 153B, 235 (1985).
- 37) P. W. Lisowski et al., Phys. Rev. Lett. 49, 255 (1982).

REFERENCES (Section II)

1. P. Dalpiaz et al., CERN/ECFA/72/4, Vol. I, p. 284; CERN proposal SPSC/p. 87, July 1977.
2. D. Underwood et al., A Polarized Beam for the M-3 Line (Fermilab), ANL-HEP-PR-78-05.
3. J. W. Cronin and O. E. Overseth, Phys. Rev. 129, 1795 (1963);
O. E. Overseth et al., Phys. Rev. Lett. 19, 391 (1967).
4. H. Primakoff, Phys. Rev. 81, 899 (1951).
5. D. G. Underwood, ANL-HEP-PR-77-56.

DISCLAIMER

This report was prepared as an account of work sponsored by an agency of the United States Government. Neither the United States Government nor any agency thereof, nor any of their employees, makes any warranty, express or implied, or assumes any legal liability or responsibility for the accuracy, completeness, or usefulness of any information, apparatus, product, or process disclosed, or represents that its use would not infringe privately owned rights. Reference herein to any specific commercial product, process, or service by trade name, trademark, manufacturer, or otherwise does not necessarily constitute or imply its endorsement, recommendation, or favoring by the United States Government or any agency thereof. The views and opinions of authors expressed herein do not necessarily state or reflect those of the United States Government or any agency thereof.